[PS]Paleogeography, Burial History, Porosity Development, and 35 Years of Production History from the Middle Devonian Slave Point Formation at Slave Field, Near the Peace River Arch, Alberta*

John B. Dunham[1] and Nigel Watts[2]

Search and Discovery Article #51323 (2016)**
Posted October 31, 2016

*Adapted from poster presentation given at AAPG 2016 Annual Convention and Exhibition, Calgary, Alberta, Canada, June 19-22, 2016

[1]Dunham Consulting, Ventura, California, United States (johndunham76@gmail.com)
[2]Bernum Petroleum Ltd, Calgary, Alberta, Canada (nwatts@shaw.ca)

Abstract

Cores from Slave Field recover Precambrian granite basement. During the Middle Devonian, the Peace River Arch was an expanse of granite highlands flanked by alluvial plains. Slave Field cores show granite basement overlain by variable thicknesses of alluvial Granite-Wash sand, followed by marine carbonate sediment of the Givetian-age Slave Point Formation. The paleo-topographic surface formed by hills and valleys on the irregular granite surface forms the major control on the types of carbonate facies that overlie basement. In topographic lows, alluvial Granite Wash sand is relatively thick above basement, and the first carbonate sediments deposited by incipient marine onlap are laminated peritidal muds. As marine-onlap continued, the higher flanks of granite hills were flooded by deeper-marine carbonate facies types that contain fossils including the stick-shaped stromatoporoid *Amphipora* as well as tabular and bulbous stromatoporoids. These fossils are particularly susceptible to dissolution during burial diagenesis, and the reservoir quality of the Slave Point Formation is directly related to presence or absence of these soluble components. The final phase of marine onlap resulted in deposition of a “death assemblage” of crinoid-brachiopod floatstone above a firm-ground on top of the shallow-marine Slave Point platform. There is no evidence of karsting on the top of the Slave Point platform. During burial, the paragenetic sequence progressed from dolomite-replacement of lime-mud matrix, but not fossils, which remained calcium carbonate, followed by stylolites and associated compaction fractures, followed by dissolution of calcite fossils but not dolomite-mud matrix, followed by precipitation of coarse vug-lining saddle dolomite, followed by very coarse crystalline late calcite cement, and ultimately oil-migration into the moldic-porosity system. Shale compaction curves and bottom-hole temperatures constrain the basin model, and show that potential source rocks are immature at Slave field; the oil has migrated from deeper kitchens to the southwest. Maximum burial depth is estimated at about 3000 meters, followed by about 1500 meters of tectonic uplift beginning in the Cretaceous. Maximum temperature at base Slave Point is estimated to be about 100 °C. The field has produced over 11.4 million barrels of oil. Core data combined with 35 years of production statistics convey lessons that are relevant to ongoing exploration and production in the region.

References Cited

Bachu, S., and R.A. Burwash, 1994, Geothermal Regime in the Western Canada Sedimentary Basin, Geological Atlas of the Western Canada Sedimentary Basin: in G.D. Mossop and I. Shetsen (comp.): Canadian Society of Petroleum Geologists and Alberta Research Council, Chapter 30, p. 447-454.

Bell, J.S., P.R. Price, and P.J. McLellan, 1994, In-situ stress in the Western Canada Sedimentary Basin, Geological Atlas of the Western Canada Sedimentary Basin: in G.D. Mossop and I. Shetsen (comp.): Canadian Society of Petroleum Geologists and Alberta Research Council, Chapter 29, p. 439-446.

Bouzidi, Y., D.R. Schmitt, R.A. Burwash, and E.R. Kanasewich, 2002, Depth migration of deep seismic reflection profiles: crustal thickness variations in Alberta: Canadian Journal of Earth Sciences, v. 39, p. 331-350.

Chambers, J., W. Cleveland, B. Kleiner, and P. Tukey, 1983, Graphical Methods for Data Analysis: Wadsworth Statistics/Probability Series, Duxbury Press, Boston, 395 p.

Creaney, S., J. Allan, K.S. Cole, M.G. Fowler, P.W. Brooks, K.G. Osadetz, R.W. Macqueen, L.R. Snowdon, and C.L. Riediger, 1994, Petroleum generation and migration in the Western Canada Sedimentary Basin: in Mossop, G.D., and Shetsen, I., eds., Geological Atlas of the Western Canada Sedimentary Basin: Canadian Society of Petroleum Geologists and Alberta Research Council, p. 455–468.

Ferry, R.M., 1989, Beaverhill Lake Group Carbonate Reservoirs: in Hills, L.V., and Cederwall, D.A., eds., Geophysical Atlas of Western Canadian Hydrocarbon Pools: Canadian Society of Exploration Geophysicists / Canadian Society of Petroleum Geologists Atlas Series, Chapter 3, p. 67-99.

Haq, B.U., and S.R. Schutter, 2008, A chronology of Paleozoic sea-level changes: Science, v. 322, p. 64-68.

Ogg, J.G., G. Ogg, and F.M. Gradstein, 2008, Paleozoic Time Scale and Sea-Level History: The Concise Geologic Time Scale, Cambridge University Press, 178 p.

Snedden, J.W., and C. Liu, 2010, A compilation of Phanerozoic sea-level change, coastal onlaps, and recommended sequence designations: Search and Discovery Article #40594, Accessed October 23, 2016, http://www.searchanddiscovery.com/pdfz/documents/2010/40594snedden/ndx_snedden.pdf.html

Weides, S., 2014, Exploration of geothermal resources in the Alberta Basin, Canada: Ph.D. Dissertation, Technical University of Berlin, 130 p.

Wright, G.N., M.E. McMechan, and D.E.G. Potter, 1994, Structure and Architecture of the Western Canada Sedimentary Basin, Geological Atlas of the Western Canada Sedimentary Basin: in G.D. Mossop and I. Shetsen (comp.): Canadian Society of Petroleum Geologists and Alberta Research Council, Chapter 3, p. 25-40.

Paleogeography, Burial History, Porosity Development, and 35 Years of Production History from the Middle Devonian Slave Point Formation at Slave Field, Near the Peace River Arch, Alberta

John Dunham, Ventura CA johndunham76@gmail.com
Nigel Watts, Calgary AB nwatts@shaw.ca

ABSTRACT

Since 1980, the Slave Point S-Pool has produced more than 11.5 million barrels of light oil (~35° API), but always with high water cut (45.6 million barrels water). Moldic porosity accounts for almost all of the effective porosity in the Slave Point reservoir. The molds formed from selective dissolution of fossil constituents including brachiopod shells, bulbous and tabular stromatoporoid masses, and fragments of the stromatoporoid genus Amphipora. These grains are enclosed in a matrix of light-gray microcrystalline dolomite, which is interpreted as a diagenetic replacement of original lime micrite. The microcrystalline dolomite has no effective porosity and is impermeable; consequently, reservoir permeability is dependent on touching and interconnection of fossil molds, and also on vertical fractures that appear to result from vertical compaction rather than tectonic compression. Thus, although the porosity is diagenetic in origin, the porosity, permeability, and oil production are all controlled by original depositional carbonate facies.

Carbonate Sediments: Five general carbonate facies types are present in the Slave Point reservoir: Facies 1 = Crinoid-Brachiopod Floatstone, Facies 2 = Tabular and Bulbous Stromatoporoid Boundstone, Facies 3 = Amphipora Rudstone to Floatstone, Facies 4 = Dolomite Mudstone; and Facies 5 = Bioclast Grainstone-Packstone. At some locations these carbonates overly Facies 6 which is Granite Wash Sand, while at other locations these carbonates lie directly on top of red Precambrian-Granite Basement. The vertical arrangement of these facies records an overall relative marine onlap, with Precambrian Basement hills fringed by alluvial fans of Granite Wash sand that are then inundated by the leading edge of seawater encroachment leading to deposition of marginal marine carbonates.

Carbonate Reservoirs: Each of the different facies types is characterized by a different fossil assemblage, and some fossils are more susceptible to dissolution than others. Effective porosity is formed by moldic pores that formed by leaching of certain fossil fragments. The moldic pores are classed as either touching, or not touching. Whole-core permeability measurements document that only the touching pore classes produce significant permeability in the Slave Field reservoir. Some facies types contain more touching moldic pores than other facies types.

Origin of Porosity: The western edge of the Western Canada Sedimentary Basin reached greatest burial depth during emplacement of the Cordilleran Fold and Thrust Belt in the Late Mesozoic. Hot formation water migrated up-dip from the deep basin within permeable rocks of the Basement and the Basal Clastic Unit at the contact between Precambrian Basement and Paleozoic sediment. This fluid did not dissolve the microcrystalline dolomite matrix, but it did dissolve any calcite grains that it was able to touch. Regional migration took place at the Basement – Paleozoic contact; local migration within the insoluble dolomite matrix took place along "dissolution fronts", as corrosion advanced from calcite-fossil-fragment to adjacent calcite-fossil-fragment wherever the grains touched one another. Fractures that formed along stylolites also facilitated corrosive-fluid migration. Calcite grains dissolved to form moldic pores wherever corrosive fluid was able to reach them. However, there are areas where unleached calcite fossils are encased in microcrystalline dolomite matrix. These fossils did not dissolve because the corrosive fluid could not reach them, since the dissolution front cannot propagate through impermeable microcrystalline-dolomite matrix. The dissolution front proceeds from touching-fossil to touching-fossil, and along stylolite fractures, but isolated pods of unleached calcite can be left behind. The porosity forms by dissolution of calcite grains that are contacted by corrosive fluids that migrated up-dip from the deep basin. Dissolution took place before, and probably shortly before, oil migration.

Slave Field Production History: Slave Field is a Water Drive Reservoir. Water surrounds the reservoir on all sides. In many wells on the flanks of the field, the oil-water contact is present within the Slave Point Formation, making it necessary to carefully select zones to perforate that are not too close to the oil-water contact. As oil production took place over the years, the original oil-water contact rose up within the reservoir, eventually reaching the production perforations. Most wells initially produced oil with no or low water cut. Onset of high water cut varies from well to well. Early water cut can result from vertical coning of bottom-water in high-permeability zones that were perforated near the oil-water contact. Early water in some wells may be related to poor cement-bond between formation and cement outside the casing, which would allow water to flow outside the casing and enter perforations located above the oil-water contact in the reservoir. Wells located in the structurally highest positions in the reservoir have perforations that are highest above the original oil-water contact, and these are the wells that had the longest periods of oil production with low water cut. The first water to reach these wells is edge-water that has channeled laterally up-dip as the rising water contact reached high-permeability zones. High-permeability vuggy zones are susceptible to channeling, such that "edge-water" is pulled up these zones before the "bottom-water" from the rising water contact reaches the producing perforations.

Lessions Learned: 1) The best reservoir rocks in Slave Field are on the mid to upper flanks of Basement Highs, while poor quality rocks make up the thick peritidal intervals in valleys between the Basement Highs. 2) Try to avoid drilling through the oil-water contact within the reservoir in order to avoid the possibility of channeling water behind casing in wells with poor cement bonds. 3) Do not perforate high permeability zones that are within a few meters of the oil-water contact, in order to reduce the effects of channeling of bottom-water and edge-water in high-permeability zones. 4) Do not respond to onset of water by increasing the pumping rate of the well; increased pumping rate encourages channeling of edge-water up through high permeability zones. Slave Point exploration continues in Alberta and B.C., therefore information from this presentation are relevant to 21th Century Slave Point Exploration and Production.

References –

Bachu, S., and Burwash, R.A., 1994, Geothermal Regime in the Western Canada Sedimentary Basin, Geological Atlas of the Western Canada Sedimentary Basin, in G.D. Mossop and I. Shetsen (comp.): Canadian Society of Petroleum Geologists and Alberta Research Council, Chapter 30, p. 447-454.

Bell, J.S., Price, P.R., and McLellan, PJ, 1994, In-situ stress in the Western Canada Sedimentary Basin, Geological Atlas of the Western Canada Sedimentary Basin, in G.D. Mossop and I. Shetsen (comp.): Canadian Society of Petroleum Geologists and Alberta Research Council, Chapter 29, p. 439-446.

Bouzidi, Y., Schmitt, D.R., Burwash, R.A., and Kanasewich, E.R., 2002, Depth migration of deep seismic reflection profiles: crustal thickness variations in Alberta: Canadian Journal of Earth Sciences, v. 39, p. 331-350.

Chambers, J., Cleveland, W., Kleiner, B., Tukey, P., 1983, Graphical Methods for Data Analysis: Wadsworth Statistics/Probability Series, Duxbury Press, Boston, 395 p.

Creaney, S., Allan, J., Cole, K.S., Fowler, M.G, Brooks, P.W., Osadetz, K.G., Macqueen, R.W., Snowdon, L.R., Riediger, C.L., 1994, Petroleum generation and migration in the Western Canada Sedimentary Basin, in Mossop, G.D., and Shetsen, I., eds., Geological Atlas of the Western Canada Sedimentary Basin: Canadian Society of Petroleum Geologists and Alberta Research Council, p. 455–468.

Ferry, R. M., 1989, Beaverhill Lake Group Carbonate Reservoirs, in Hills, L.V., and Cederwall, D.A., eds., Geophysical Atlas of Western Canadian Hydrocarbon Pools: Canadian Society of Exploration Geophysicists / Canadian Society of Petroleum Geologists Atlas Series, Chapter 3, p. 67-99.

Haq, B.U., and Schutter, S.R., 2008, A chronology of Paleozoic sea-level changes: Science, v. 322, p. 64-68.

Ogg, J.G., Ogg, G., and Gradstein, F.M., 2008, Paleozoic Time Scale and Sea-Level History: The Concise Geologic Time Scale, Cambridge University Press, 178 p.

Snedden, J.W., and Liu, C., 2010: A compilation of Phanerozoic sea-level change, coastal onlaps, and recommended sequence designations: American Association of Petroleum Geologists, Search and Discovery Article #40594.

Weides, S., 2014, Exploration of geothermal resources in the Alberta Basin, Canada: Ph.D. Dissertation, Technical University of Berlin, 130 p.

Wright, G.N., McMechan, M.E., and Potter, D.E.G., 1994, Structure and Architecture of the Western Canada Sedimentary Basin, Geological Atlas of the Western Canada Sedimentary Basin, in G.D. Mossop and I. Shetsen (comp.): Canadian Society of Petroleum Geologists and Alberta Research Council, Chapter 3, p. 25-40.

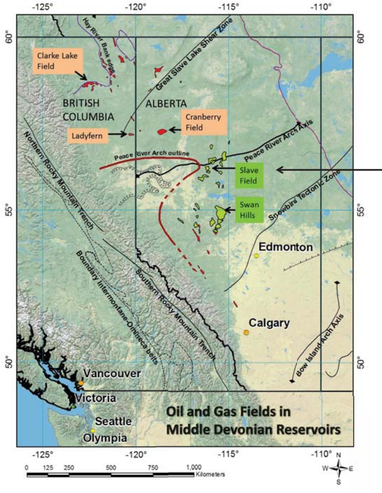

Base Slave Point Reservoir Contours Meters TVDSS: Green = Base Above Oil Water Contact At -1051.2 meters TVDSS.

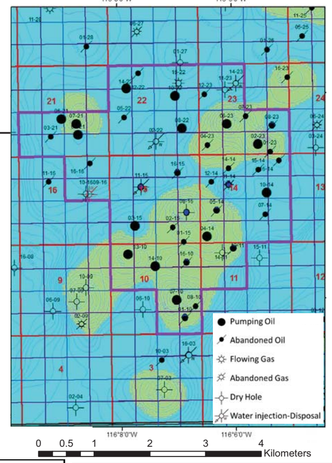

Stratigraphy at Slave Field

Period	Formation	Main Lithology	GR Log
Quat.	Glacial Drift	Conglomerate	
Cretaceous L	Peace River	Shale and Sand	
Cretaceous L	Spirit River	Shale and Sand	
Carboniferous	Shunda	Limestone and Shale	GAS
Carboniferous	Banff	Limestone and Shale	
Devonian U	Wabamun	Dolomite and Limestone	
Devonian U	Winterburn	Dolomite and Limestone	
Devonian U	Ireton	Shale	
Devonian U	Duverney	Shale	
Devonian U	Waterways	Shale	
Devonian M	Slave Point	Dolomite	OIL
Devonian M	Granite Wash	Dolomite	
pC	Granite		

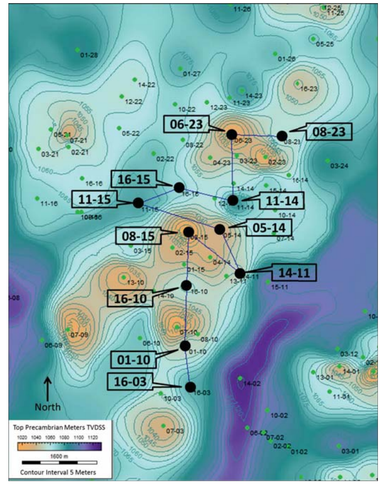

Top Granite meters TVDSS: Wells and Correlation Section

Precambrian Granite under Middle Devonian Carbonate

Dunham, 1962, and Embry and Klovan, 1972 Carbonate Textural Classes

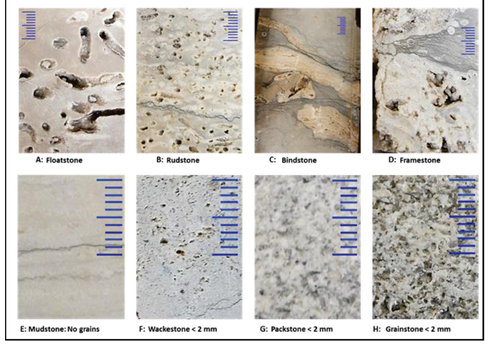

Common Devonian Fossils within the Slave Point Formation at Slave Field

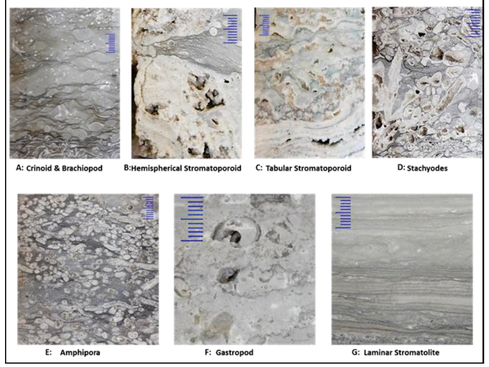

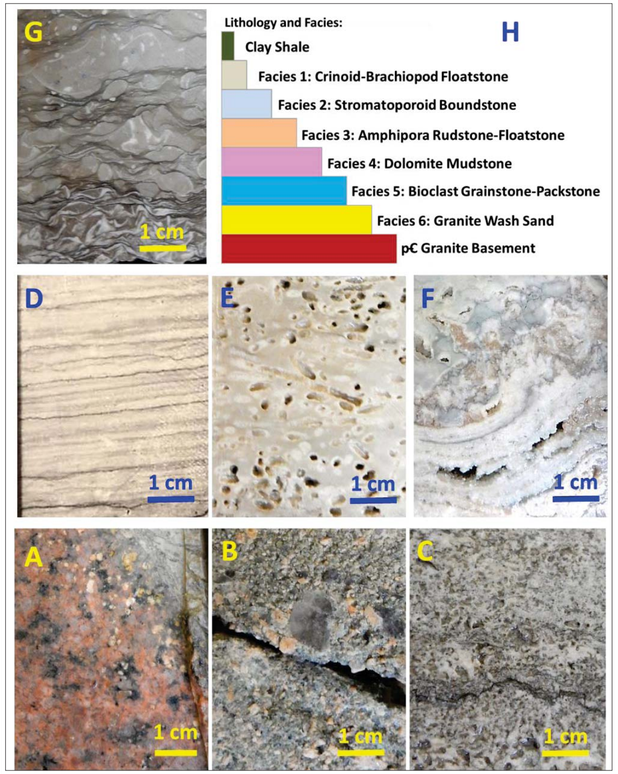

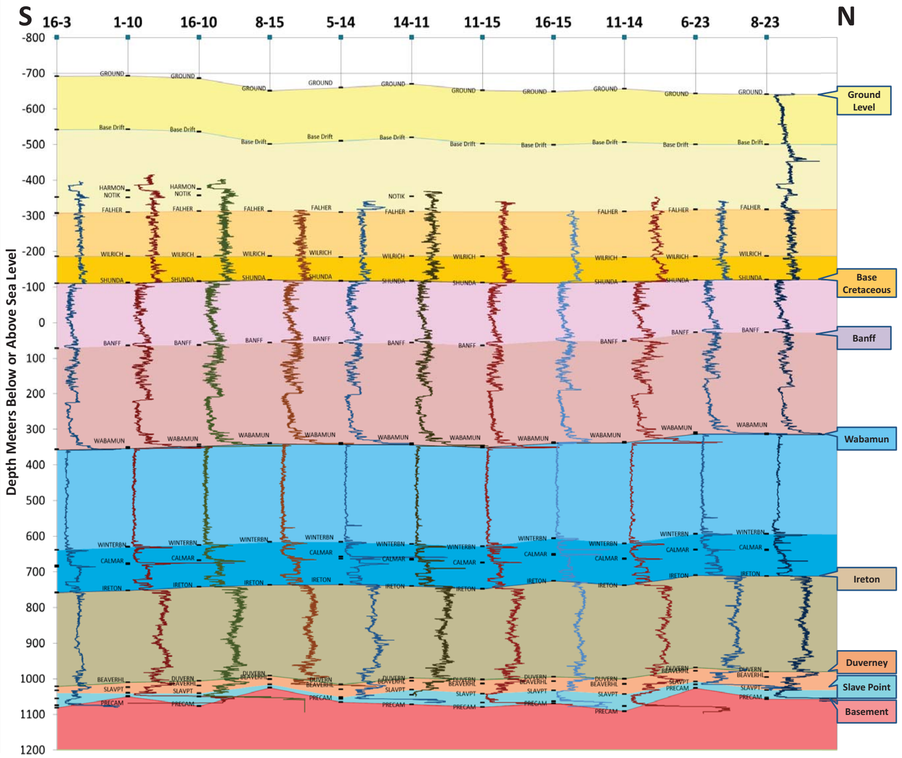

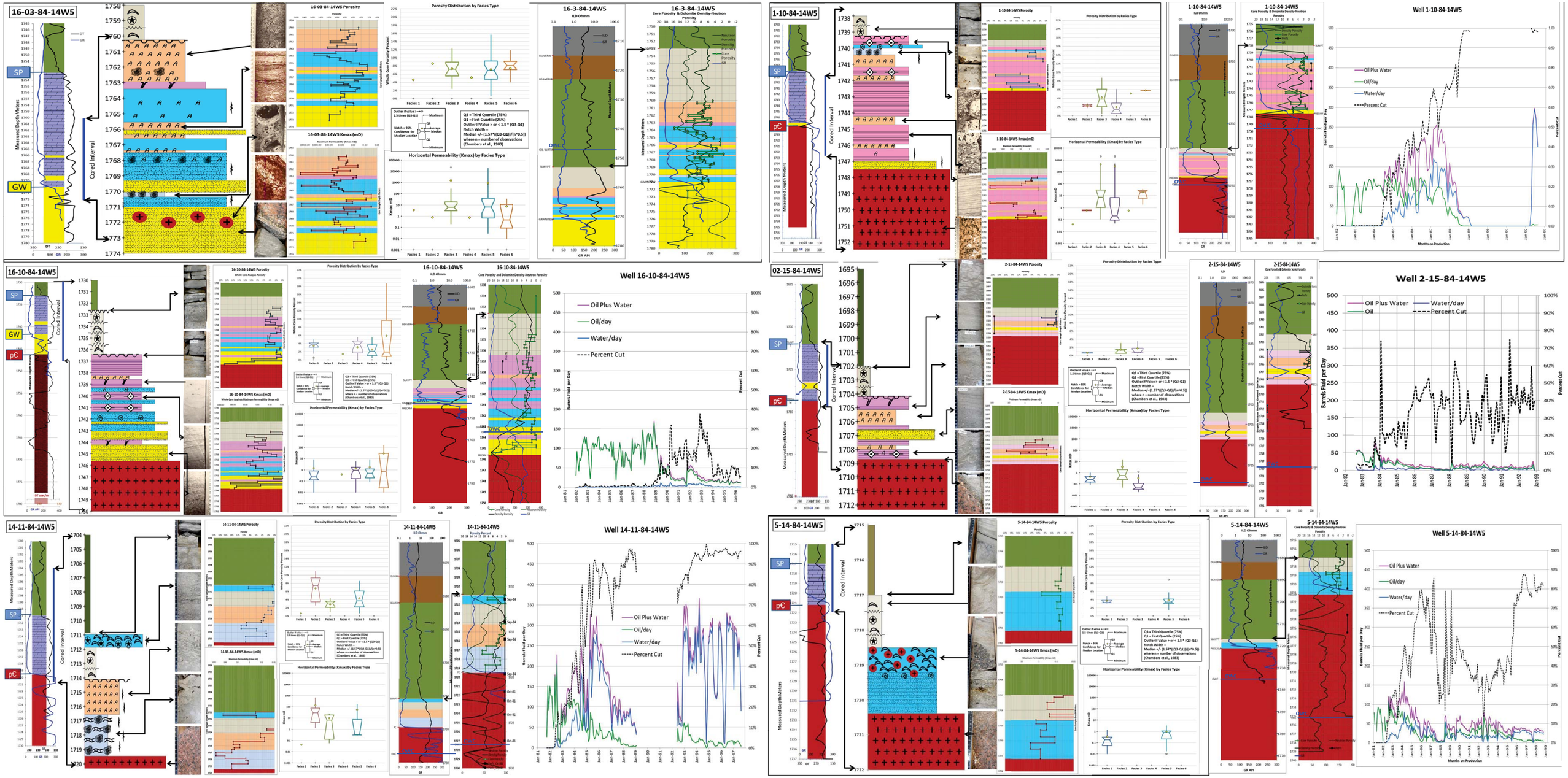
16-03-84-14W5
16-03-84-14W5 Porosity
Porosity Distribution by Facies Type
16-03-84-14W5 Kmax (mD)
Horizontal Permeability (Kmax) by Facies Type
16-3-84-14W5
16-3-84-14W5
1-10-84-14W5
1-10-84-14W5 Porosity
Porosity Distribution by Facies Type
1-10-84-14W5 Kmax (mD)
Horizontal Permeability (Kmax) by Facies Type
1-10-84-14W5
1-10-84-14W5
Well 1-10-84-14W5
Oil Plus Water
Oil/day
Water/day
Percent Cut
Months on Production
16-10-84-14W5
16-10-84-14W5 Porosity
Porosity Distribution by Facies Type
16-10-84-14W5 Kmax (mD)
Horizontal Permeability (Kmax) by Facies Type
16-10-84-14W5
16-10-84-14W5
Well 16-10-84-14W5
Oil Plus Water
Oil/day
Water/day
Percent Cut
02-15-84-14W5
2-15-84-14W5 Porosity
Porosity Distribution by Facies Type
2-15-84-14W5 Kmax (mD)
Horizontal Permeability (Kmax) by Facies Type
2-15-84-14W5
2-15-84-14W5
Well 2-15-84-14W5
Oil Plus Water
Oil
Water/day
Percent Cut
14-11-84-14W5
14-11-84-14W5 Porosity
Porosity Distribution by Facies Type
14-11-84-14W5 Kmax (mD)
Horizontal Permeability (Kmax) by Facies Type
14-11-84-14W5
14-11-84-14W5
Well 14-11-84-14W5
Oil Plus Water
Oil/day
Water/day
Percent Cut
5-14-84-14W5
5-14-84-14W5 Porosity
Porosity Distribution by Facies Type
5-14-84-14W5 Kmax (mD)
Horizontal Permeability (Kmax) by Facies Type
5-14-84-14W5
5-14-84-14W5
Well 5-14-84-14W5
Oil Plus Water
Oil/day
Water/day
Percent Cut
Months on Production

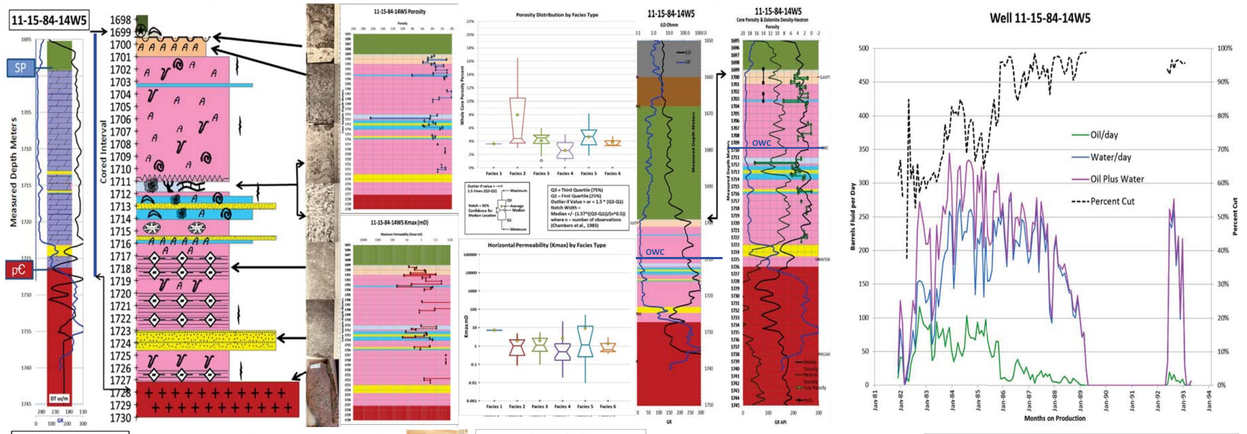
11-15-84-14W5
Measured Depth Meters
Cored Interval
SP
pC
OWC
11-15-84-14W5 Porosity
Porosity Distribution by Facies Type
11-15-84-14W5 Kmax(mD)
Horizontal Permeability (Kmax) by Facies Type
11-15-84-14W5
ILD Ohms
Core Porosity & Dolomite Density-Neutron Porosity
Well 11-15-84-14W5
Oil/day
Water/day
Oil Plus Water
Percent Cut
Barrels Fluid per Day
Months on Production

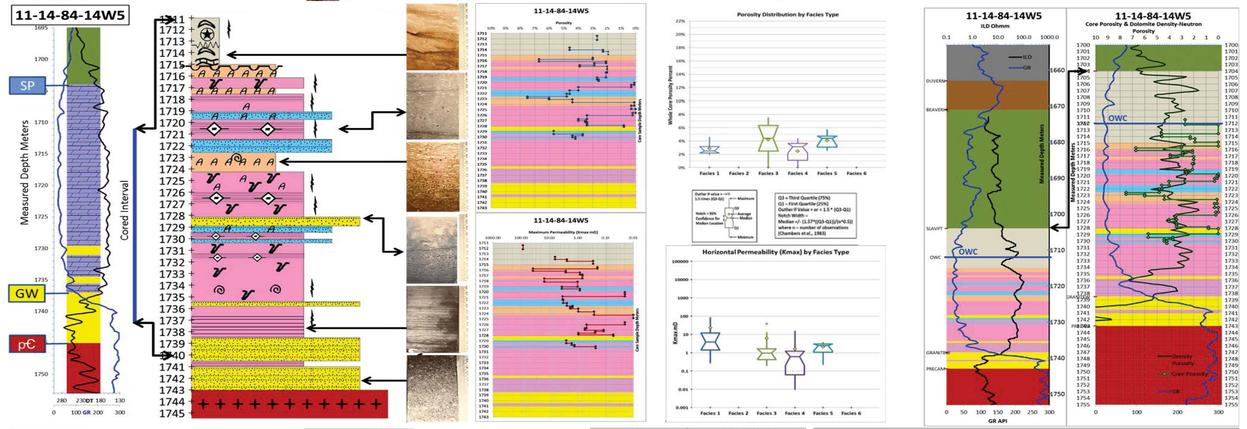
11-14-84-14W5
Measured Depth Meters
Cored Interval
SP
GW
pC
OWC
11-14-84-14W5
Porosity Distribution by Facies Type
Horizontal Permeability (Kmax) by Facies Type
ILD Ohmm
Core Porosity & Dolomite Density-Neutron Porosity

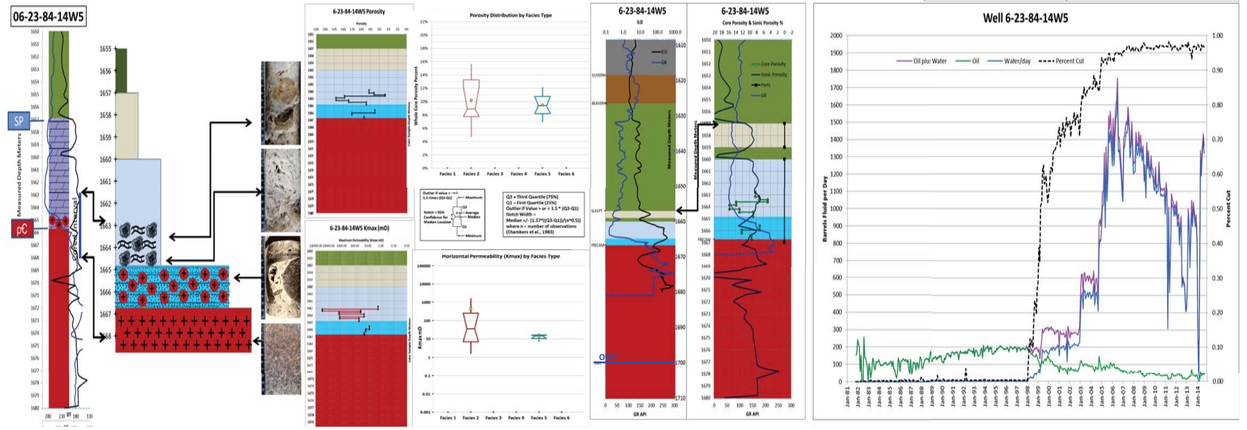
06-23-84-14W5
Measured Depth Meters
Cored Interval
SP
pC
OWC
6-23-84-14W5 Porosity
Porosity Distribution by Facies Type
6-23-84-14W5 Kmax(mD)
Horizontal Permeability (Kmax) by Facies Type
6-23-84-14W5
ILD
Core Porosity & Sonic Porosity %
Well 6-23-84-14W5
Oil plus Water
Oil
Water/day
Percent Cut
Barrels Fluid per Day

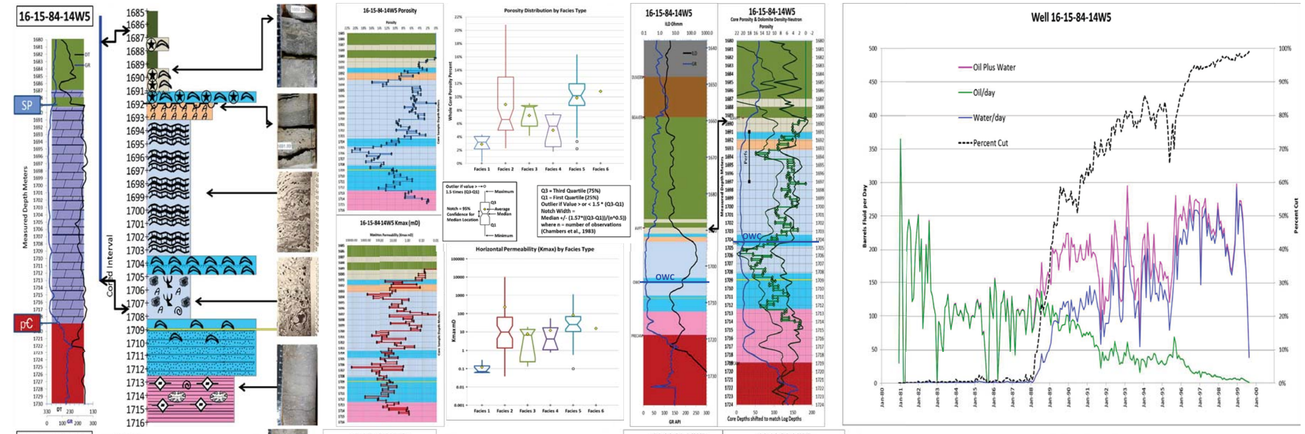
16-15-84-14W5
Measured Depth Meters
Cored Interval
SP
pC
OWC
16-15-84-14W5 Porosity
Porosity Distribution by Facies Type
16-15-84-14W5 Kmax(mD)
Horizontal Permeability (Kmax) by Facies Type
16-15-84-14W5
ILD Ohms
Core Porosity & Dolomite Density-Neutron Porosity
Well 16-15-84-14W5
Oil Plus Water
Oil/day
Water/day
Percent Cut
Barrels Fluid per Day

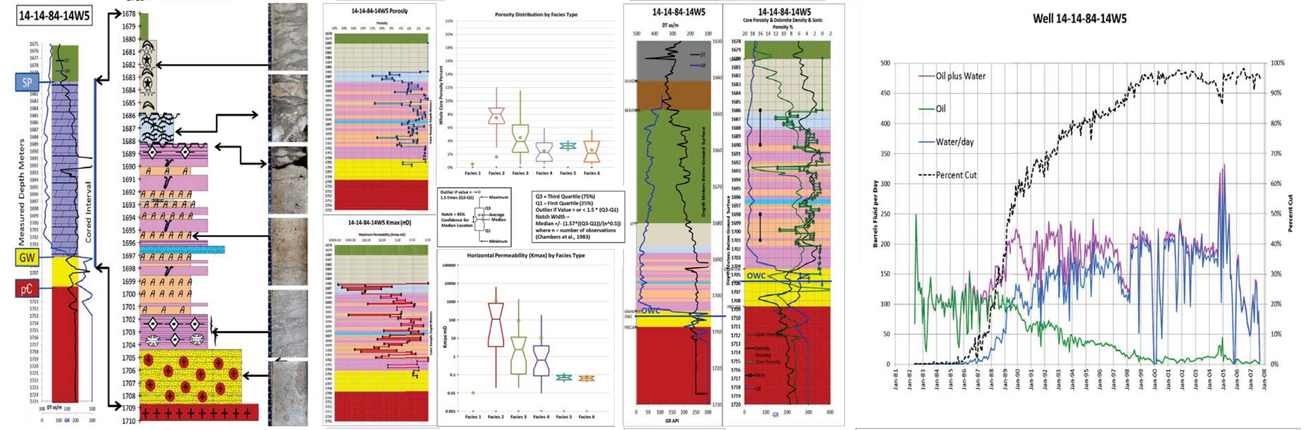
14-14-84-14W5
Measured Depth Meters
Cored Interval
SP
GW
pC
OWC
14-14-84-14W5 Porosity
Porosity Distribution by Facies Type
14-14-84-14W5 Kmax(mD)
Horizontal Permeability (Kmax) by Facies Type
14-14-84-14W5
DT us/m
Core Porosity & Dolomite Density & Sonic Porosity %
Well 14-14-84-14W5
Oil plus Water
Oil
Water/day
Percent Cut
Barrels Fluid per Day

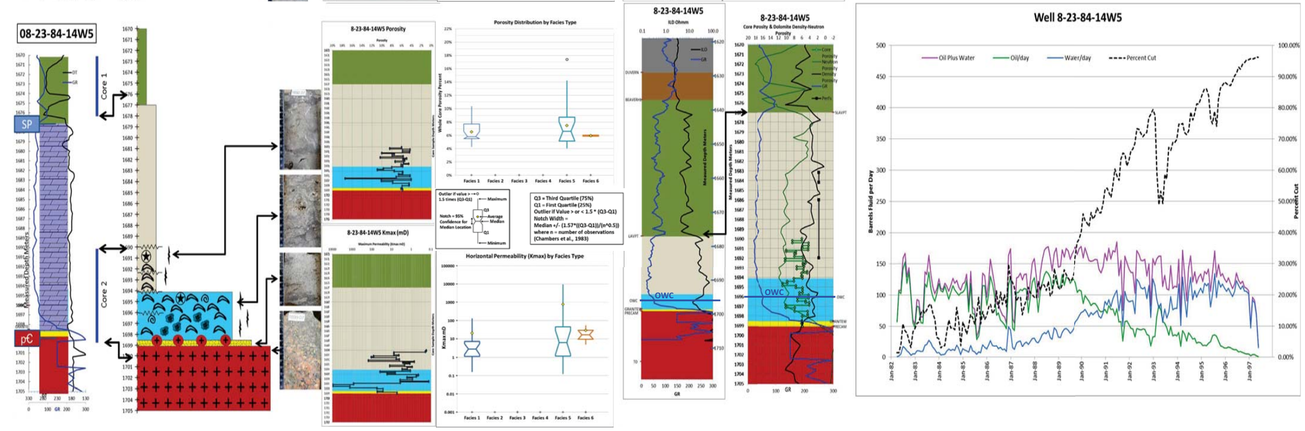
08-23-84-14W5
Measured Depth Meters
Cored Interval
Core 1
Core 2
SP
pC
OWC
8-23-84-14W5 Porosity
Porosity Distribution by Facies Type
8-23-84-14W5 Kmax(mD)
Horizontal Permeability (Kmax) by Facies Type
8-23-84-14W5
ILD Ohmm
Core Porosity & Dolomite Density-Neutron Porosity
Well 8-23-84-14W5
Oil Plus Water
Oil/day
Water/day
Percent Cut
Barrels Fluid per Day

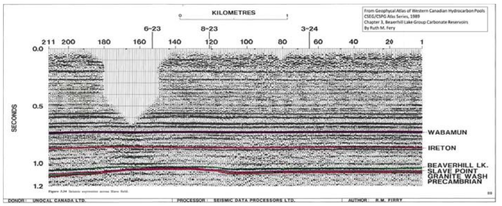

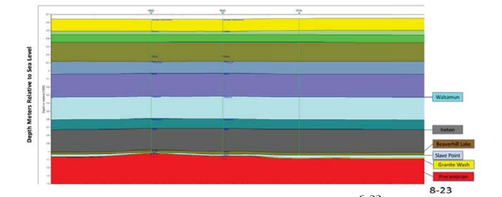

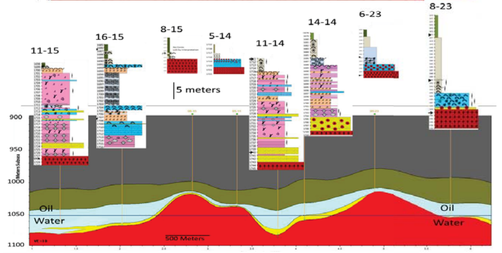

Correlation Section Illustrating Influence of Basement Topography on Slave Point Sediments

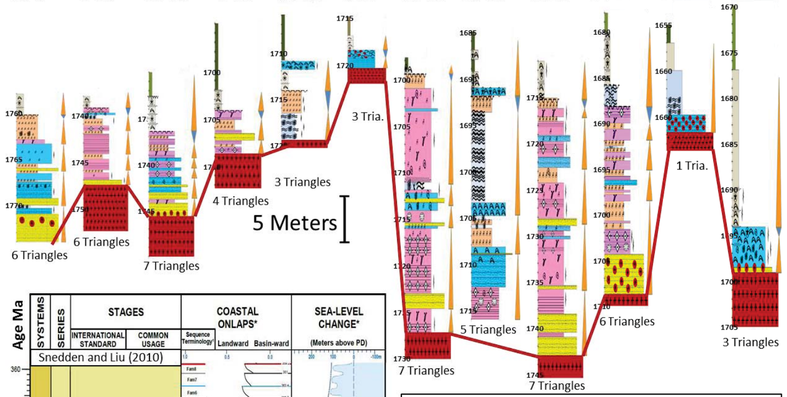

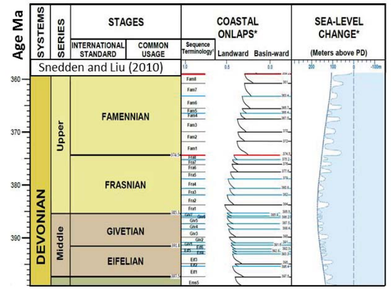

Snedden and Liu (2010) compilation of sea-level change and coastal onlap curves including Haq et al. (1987) and Ogg and Ogg (2008). Slave Field bed sets record progressive onlap of granite basement highs during Givetian sea-level rise.

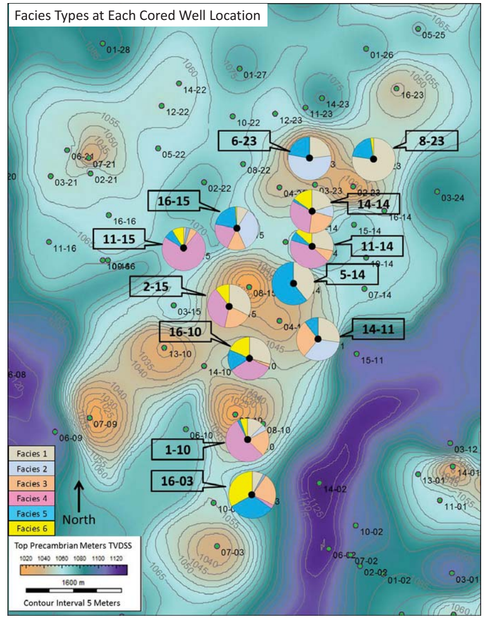

Continued onlap results in deposition of marine sediment atop granite, with little or no Granite-Wash sand at the base.

Granite-Wash is deposited in alluvial-fan and channel aprons flanking Basement Highs.

Granite-Wash alluvium in stream channels between granite hills. Initial marine onlap deposits peritidal carbonate on top of sand between hills. Further onlap would deposit marine carbonate against the flanks of the hills, directly on top of granite.

Spheroidal-Weathered granite outcrop flanked by alluvium.

Initial non-marine condition: Peace River Arch granite hills flanked by alluvial Granite-Wash sands.

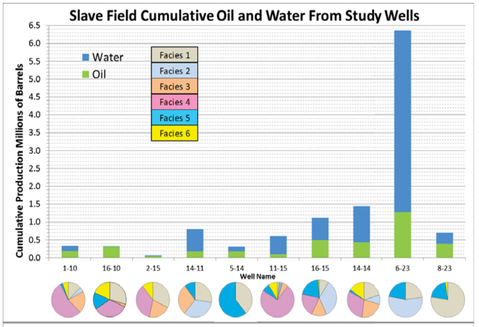

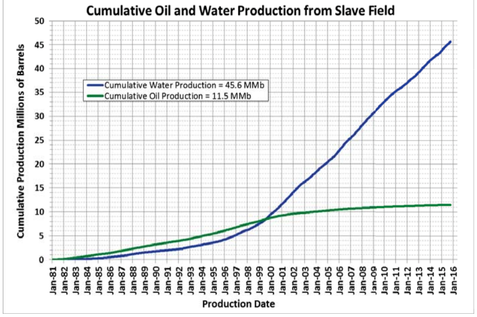

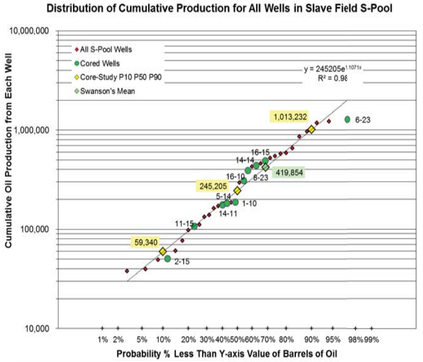

Rank	Well Name	Oil Produced	Rank	Well Name	Oil Produced
1	1-15	37,784	18	7-21	294,327
2	14-22	39,560	19	16-10	310,484
3	8-10	49,451	20	8-23	392,412
4	2-15	50,695	21	12-22	429,237
5	6-21	60,722	22	14-14	440,561
6	7-10	76,724	23	16-16	458,495
7	10-14	98,013	24	16-15	490,021
8	11-15	107,074	25	12-23	524,575
9	13-10	110,984	26	14-10	544,071
10	15-14	132,896	27	2-22	574,825
11	7-23	139,797	28	2-23	585,952
12	4-14	162,240	29	4-23	653,887
13	3-21	172,459	30	2-21	860,833
14	14-11	176,351	31	8-22	967,470
15	5-14	182,842	32	10-22	1,178,179
16	3-15	186,266	33	5-22	1,223,730
17	1-10	187,955	34	6-23	1,278,272

P-Value	Barrels Oil
P-10	59,340
P-50	245,205
P-90	1,013,232

Swanson's Mean	419,854

Oil Production from 34 wells in Slave Field follows a Lognormal Distribution. Cored wells highlighted in yellow constitute a representative sample of the population.

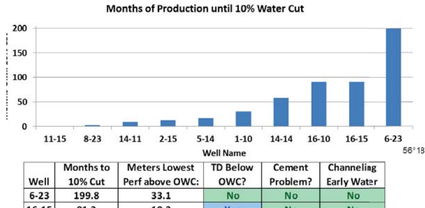

Well	Months to 10% Cut	Meters Lowest Perf above OWC:	TD Below OWC?	Cement Problem?	Channeling Early Water
6-23	199.8	33.1	No	No	No
16-15	91.3	10.3	Yes	No	No
16-10	91.3	6.6	Yes	No	No
14-14	57.8	15.8	Yes	No	No
1-10	30.4	5.6	Yes	No	No
5-14	17.2	14.7	Yes	No	Yes
2-15	12.2	5.8	Yes	No	Yes
14-11	9.1	1.3	Yes	No	Yes
8-23	3.0	4	Yes	Yes	Yes
11-15	0.1	1.9	Yes	Yes	Yes

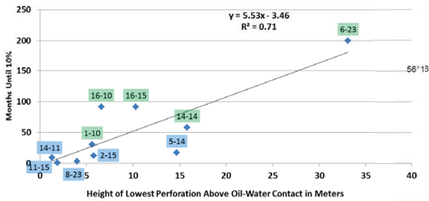

Water Production is related to factors including:
1) **Height of Perforations above Oil-Water contact.**
2) **Poor Cement Bond allowing water to flow behind casing.**
3) **Channeling of Water within high-permeability zones.**

Base Slave Point Reservoir Contours Meters TVDSS: Oil, Water and Drainage Radius; small squares are 40 acres.

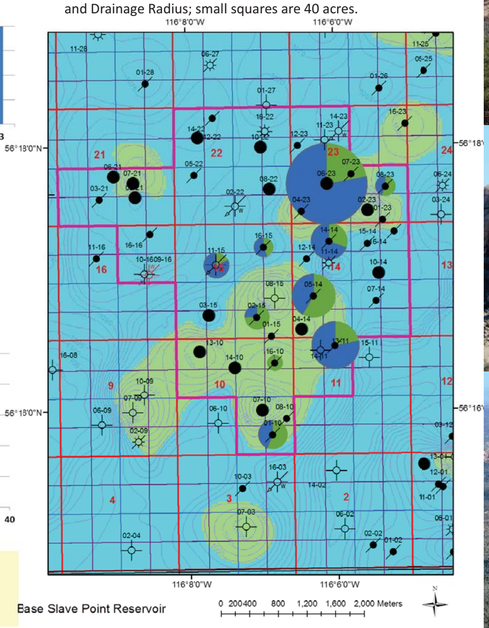

Visible Porosity Classification Example:
No Visible Porosity

Facies Type 1: Crinoid-Brachiopod Floatstone

Core 5-14-84-14W5
Sample 1: 1717.05 – 1717.15 m
Porosity: 3.1 %
Kmax: 0.04 md
K90: 0.01 md
Kv: 0.01 md

Pore Fabric: No Visible Porosity

Facies 1 Crinoid Brachiopod

Visible Porosity Classification Example:
Moldic Pores > 4 mm Not Touching

Facies Type 2: Stromatoporoid Bindstone

Core 16-15-84-14W5
Sample 54: 1702.24 – 1702.5 m
Porosity: 7.1%
Kmax: 8.0 md
K90: 7.73 md
Kv: 0.15 md

Pore Fabric: Fabric Selective leached tabular stromatoporoid.

Facies 2 Stromatoporoid

Visible Porosity Classification Example:
Moldic Pores 1 to 4 mm Touching

Facies Type 3: Amphipora Rudstone

Core 16-3-84-14W5
Sample 9: 1761.9 to 1762.15 m
Porosity: 11.6%
Kmax: 52 md
K90: 41 md
Kv: 0.03 md

Pore Fabric: Fabric Selective leached Amphipora.

Facies 3 Stick Strom

Visible Porosity Classification Example:
No Visible Porosity

Facies Type 4: Dolomite Mudstone

Core 14-14-84-14W5
Sample 62: 1739.06 – 1739.18 m
Porosity: 0.5%
Kmax: 0.03 md
K90: 0.02 md
Kv: 0.01 md

Pore Fabric: Unleached Mudstone, no porosity.

Facies 4 Mudstone

Visible Porosity Classification Example:
Moldic Pores < 1 mm Touching

Facies Type 5: Bioclast Grain-Packstone

Core 14-11-84-14W5
Sample 2: 1711.24 to 1711.33 m
Porosity: 8.5%
Kmax: 167 md
K90: 107 md
Kv: 7.71 md

Pore Fabric: Fabric Selective leached sand-sized bioclast grains.

Facies 5 Bioclast

Visible Porosity Classification Example:
Intergranular Porosity

Facies Type 6: Granite Wash Sand

Core 14-14-84-14W5
Sample 65: 1705.4 to 1705.5 m
Porosity: 3.4%
Kmax: 0.05 md
K90: 0.03 md
Kv: 0.02 md

Pore Fabric: Intergranular pore space between poorly-sorted detrital grains.

Facies 6 Granite Wash

Visible Porosity Classification Example:
Moldic Pores 1 to 4 mm Not Touching

Facies Type 1: Crinoid-Brachiopod Floatstone

Core 8-23-84-14W5
Sample 25: 1695.58 – 1695.82
Porosity: 6.6 %
Kmax: 1.6 md
K90: 0.99 md
Kv: 0.19 md

Pore Fabric: Fabric Selective leached brachiopod valves and fragments.

Facies 1 Crinoid Brachiopod

Visible Porosity Classification Example:
Moldic Pores > 4 mm Not Touching

Facies Type 2: Stromatoporoid Bindstone

Core 16-3-84-14W5
Sample 46: 1770.05 – 1770.35 m
Porosity: 11.5%
Kmax: 0.78 md
K90: 0.22 md
Kv: 0.08 md

Pore Fabric: Fabric Selective leached nodular stromatoporoids.

Facies 2 Stromatoporoid

Visible Porosity Classification Example:
Moldic Pores > 4 mm Not Touching

Facies Type 3: Stick Strom Floatstone

Core 14-14-84-14W5
Sample 39: 1690.37 – 1691.5 m
Porosity: 4.4%
Kmax: 0.07 md
K90: 0.05 md
Kv: 0.01 md

Pore Fabric: Fabric Selective leached Amphipora and nodular stroms.

Facies 3 Stick Strom

Visible Porosity Classification Example:
No Visible Porosity

Facies Type 4: Dolomite Mudstone

Core 11-14-84-14W5
Not Sampled: 1738.43 – 1738.60 m
Porosity: Not Measured
Kmax: Not Measured
K90: Not Measured
Kv: Not Measured

Pore Fabric: Unleached Mudstone, no porosity.

Facies 4 Mudstone

Visible Porosity Classification Example:
Moldic Pores < 1 mm Not Touching

Facies Type 5: Bioclast Grain-Packstone

Core 14-11-84-14W5
Sample 3: 1711.49 to 1711.58 m
Porosity: 3.7%
Kmax: 0.29 md
K90: 0.25 md
Kv: 0.09 md

Pore Fabric: Fabric Selective leached sand-sized bioclast grains.

Facies 5 Bioclast

Visible Porosity Classification Example:
Intergranular Porosity

Facies Type 6: Granite Wash Sand

Core 16-10-84-14W5
Sample 35: 1745.06 to 1745.16 m
Porosity: 14.5%
Kmax: 50 md
K90: 48.7 md
Kv: 1.07 md

Pore Fabric: Intergranular pore space between well-sorted detrital grains.

Facies 6 Granite Wash

Visible Porosity Classification Example:
Moldic Pores 1 to 4 mm Touching

Facies Type 1: Brachiopod Floatstone

Core 16-15-84-14W5
Sample 48: 1700.87 – 1701.1
Porosity: 9.2 %
Kmax: 28.5 md
K90: 10.4 md
Kv: 1.05 md

Pore Fabric: Fabric Selective leached brachiopod valves. Also Stylolite Fractures.

Facies 1 Crinoid Brachiopod

Visible Porosity Classification Example:
Moldic Pores > 4 mm Touching

Facies Type 2: Stromatoporoid Bindstone

Core 6-23-84-14W5
Sample 4: 1663.6 – 1663.86 m
Porosity: 13.7%
Kmax: 1550 md
K90: 298 md
Kv: 37.8 md

Pore Fabric: Fabric Selective leached tabular stromatoporoids.

Facies 2 Stromatoporoid

Visible Porosity Classification Example:
No Visible Porosity

Facies Type 3: Amphipora Floatstone

Core 2-15-84-14W5
Sample 9: 1705.62 – 1705.86 m
Porosity: 0.5 %
Kmax: 0.24 md
K90: 0.03 md
Kv: 0.01 md

Pore Fabric: Unleached Amphipora, no porosity.

Facies 3 Stick Strom

Visible Porosity Classification Example:
Fracture Porosity

Facies Type 4: Dolomite Mudstone

Core 8-23-84-14W5
Sample 32: 1697.51 – 1697.84
Porosity: 4.5 %
Kmax: 1280 md
K90: 9.8 md
Kv: 0.72 md

Pore Fabric: Fractures between stylolites.

Facies 4 Mudstone

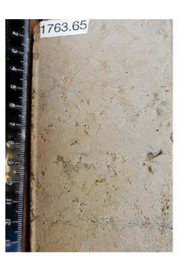

Visible Porosity Classification Example:
Moldic Pores < 1 mm Touching

Facies Type 5: Bioclast Grain-Packstone

Core 16-3-84-14W5
Sample 17: 1763.65 to 1763.9 m
Porosity: 15.6%
Kmax: 60 md
K90: 60 md
Kv: 114 md

Pore Fabric: Fabric Selective, leached sand-sized bioclasts in burrow-fill.

Facies 5 Bioclast

Visible Porosity Classification Example:
No Visible Porosity

Facies Type 6: Granite Wash Sand interlayered with Dolomite Mudstone
Core 14-14-84-14W5
Sample 64: 1703.68 to 1704.36 m
Porosity: 0.9%
Kmax: 0.04 md
K90: 0.01 md
Kv: 0.01 md

Pore Fabric: No visible porosity.

Facies 6 Granite Wash

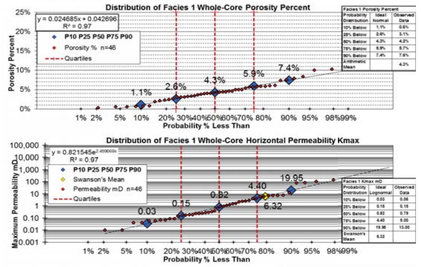

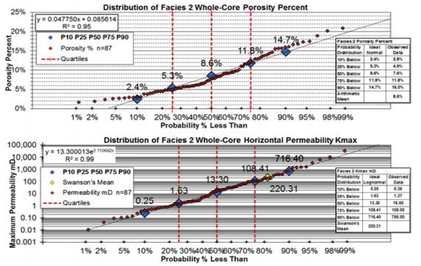

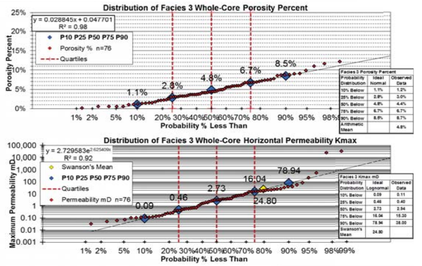

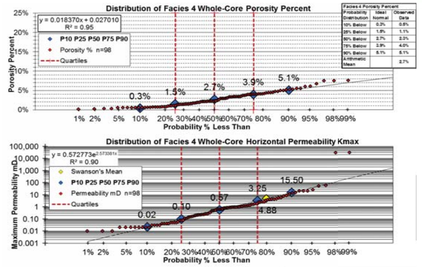

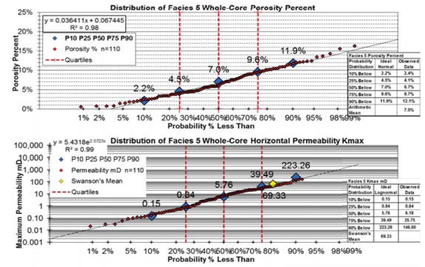

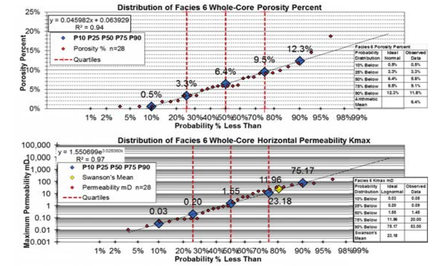

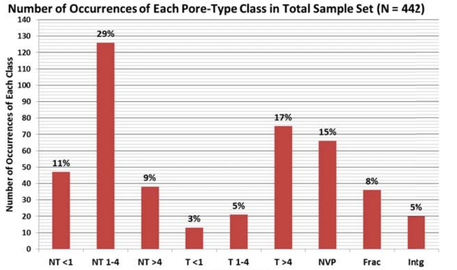

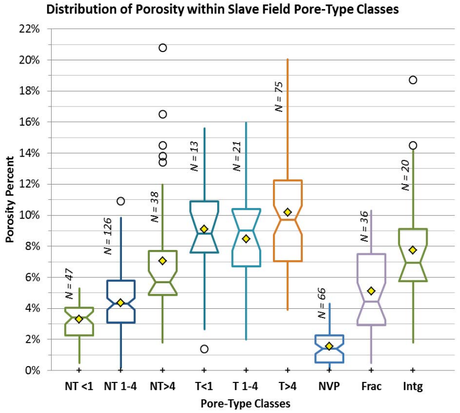

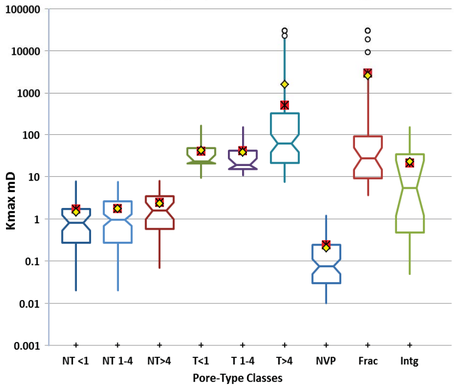

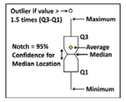

Q3 = Third Quartile (75%)
Q1 = First Quartile (25%)
Outlier if Value > or < 1.5 * (Q3-Q1)
Notch Width =
Median +/- (1.57*((Q3-Q1))/(n^0.5))
where n = number of observations
(Chambers et al., 1983)

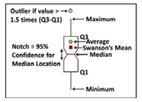

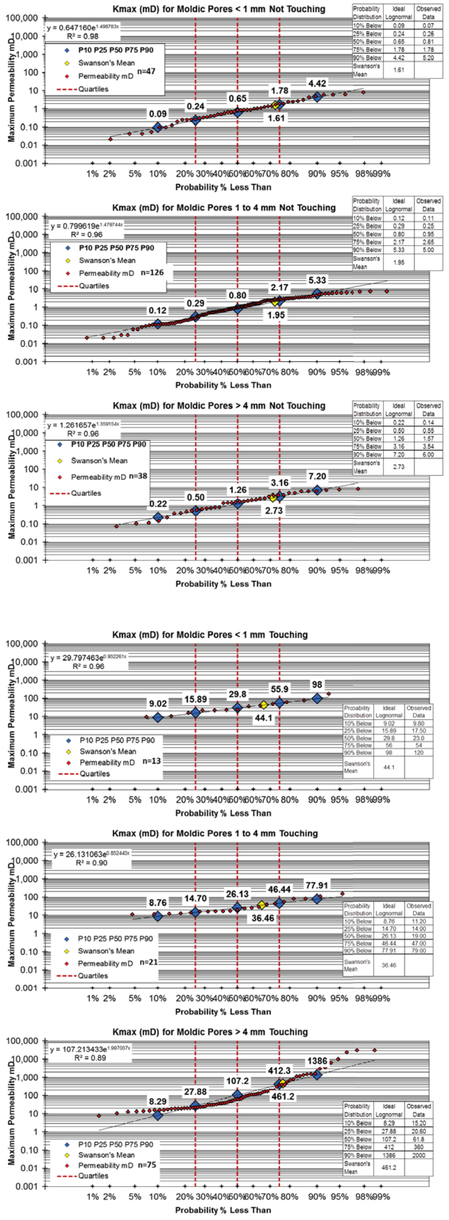

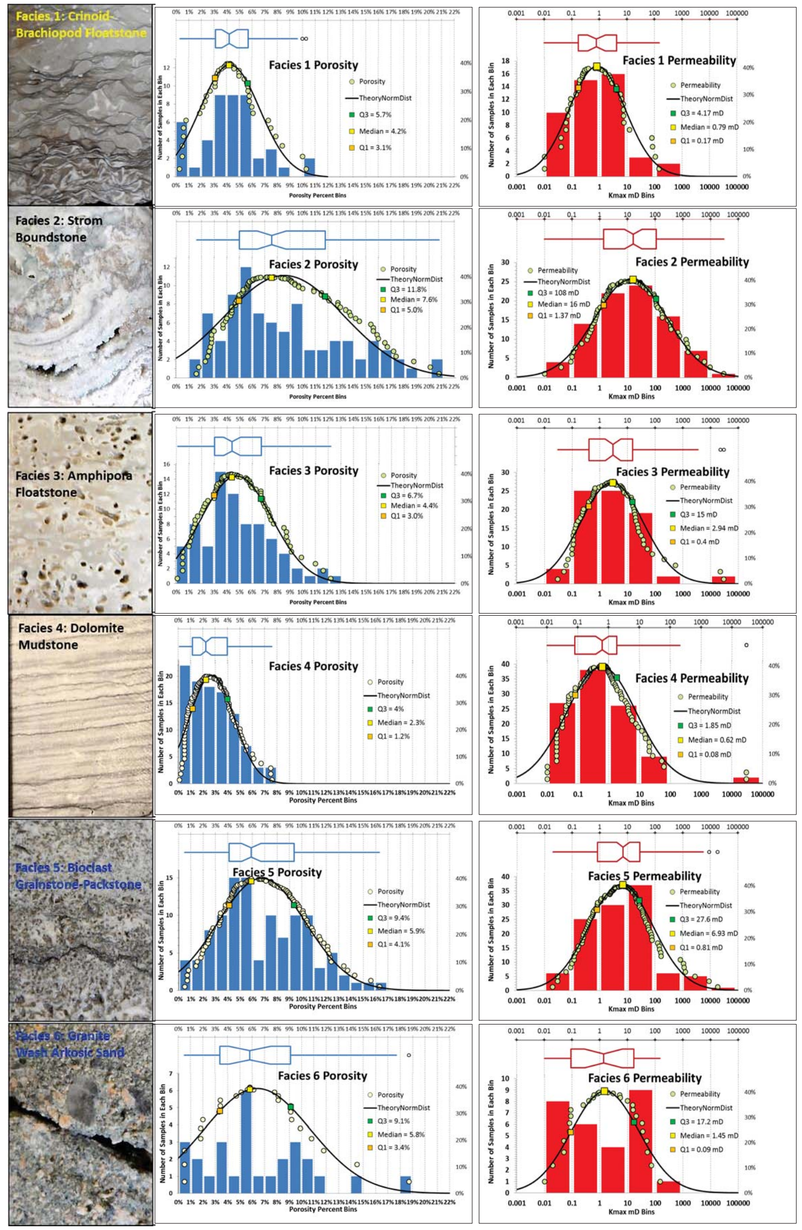

Summary Table of Porosity and Permeability in Each Facies Type -

	Porosity Percent				Permeability Kmax mD				
	P10	P50	P90	Mean	P10	P50	P90	Swanson's Mean	Reservoir Quality
Facies 1	1.1%	4.3%	7.4%	4.3%	0.03	0.82	19.95	6.32	Poor
Facies 2	2.4%	8.6%	14.7%	8.6%	0.25	13.30	716.40	220.32	Very Good
Facies 3	1.1%	4.8%	8.5%	4.8%	0.09	2.73	78.94	24.80	Fair
Facies 4	0.3%	2.7%	5.1%	2.7%	0.02	0.57	15.50	4.88	Poor
Facies 5	2.2%	7.0%	11.9%	7.0%	0.15	5.76	223.26	69.33	Good
Facies 6	0.5%	6.4%	12.3%	6.4%	0.03	1.55	75.17	23.18	Fair

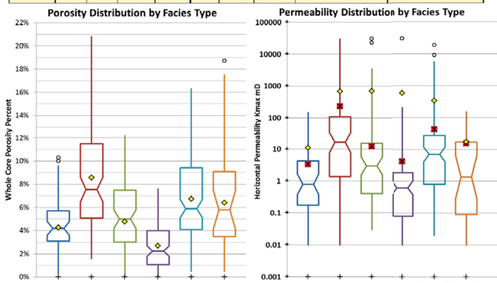

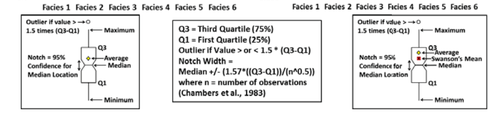

Q3 = Third Quartile (75%)
Q1 = First Quartile (25%)
Outlier if Value > or < 1.5 * (Q3-Q1)
Notch Width =
Median +/- (1.57*((Q3-Q1))/(n^0.5))
where n = number of observations
(Chambers et al., 1983)

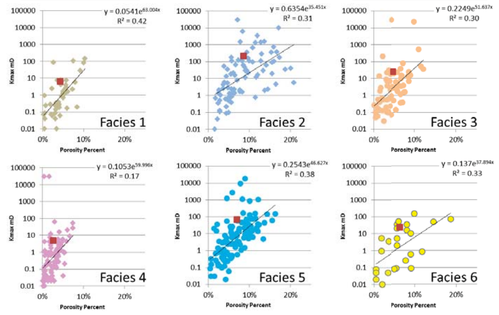

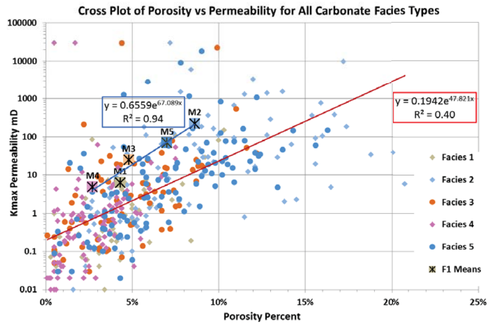

Conclusions of Exploration and Production Significance:

- Reservoir porosity and permeability are related to original depositional facies.
- More porous facies are located on the middle flanks of Basement Highs. Less porous facies are at the lower flanks of highs. Thick Slave Point interval does not necessarily correlate with good reservoir quality.
- Most dry holes in the region penetrate the top of the Slave Point Formation below the Oil-Water contact in the field.
- Some dry holes penetrate the precise top of Basement Highs, where porous carbonate is very thin or absent.
- Some wells show high water cuts earlier than other wells. Recommendation is to avoid placing perforations within a few meters of the oil-water contact. Also, problems with channeling water behind casing due to poor cement bond can be avoided by drilling development wells to total depth that is above the oil-water contact in the field.
- When wells begin to show high water cut, past practice has been to increase pumping rate in order to maintain oil production at a constant barrel per day rate. This practice promotes channeling of water within high permeability zones and may lead to even higher water cuts and therefore to lower oil-recovery factor from the well.

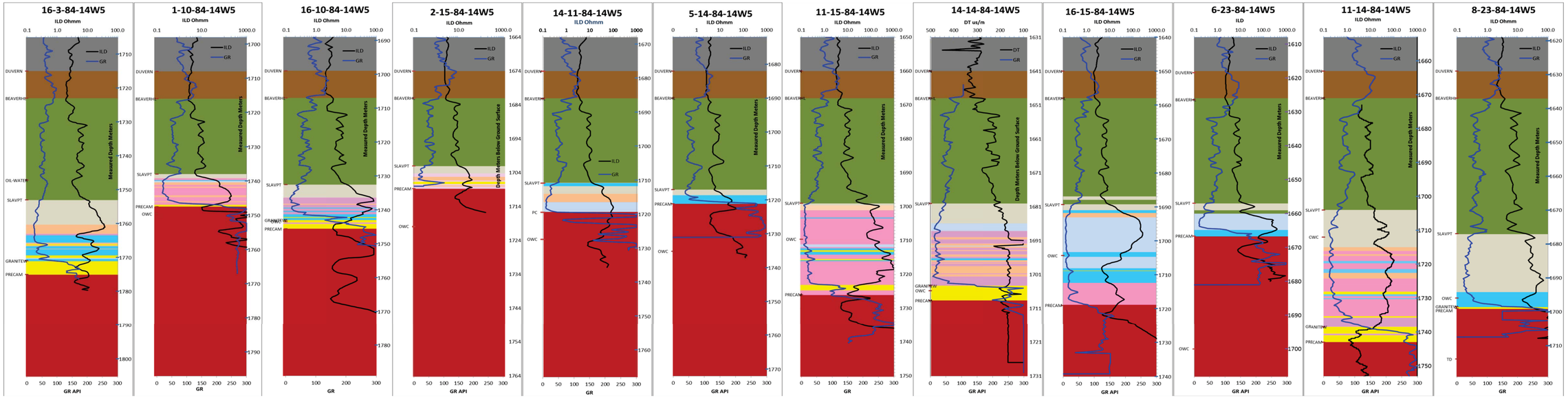

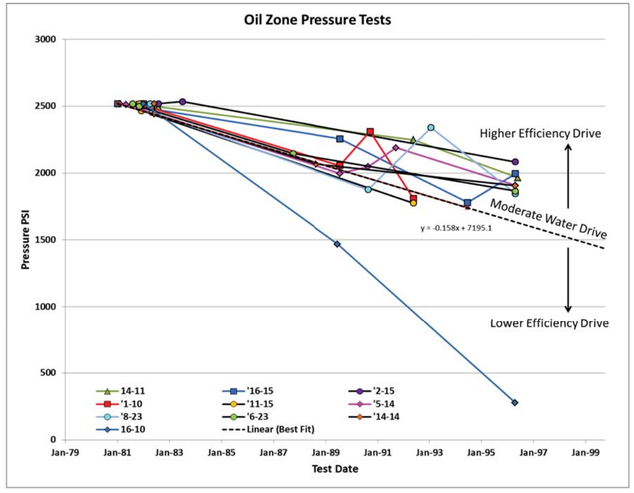

A high efficiency water drive would show little or no pressure change during production. S pool is not a high-efficiency water drive; it is a moderate to low efficiency drive. Water Injection started in 1990.

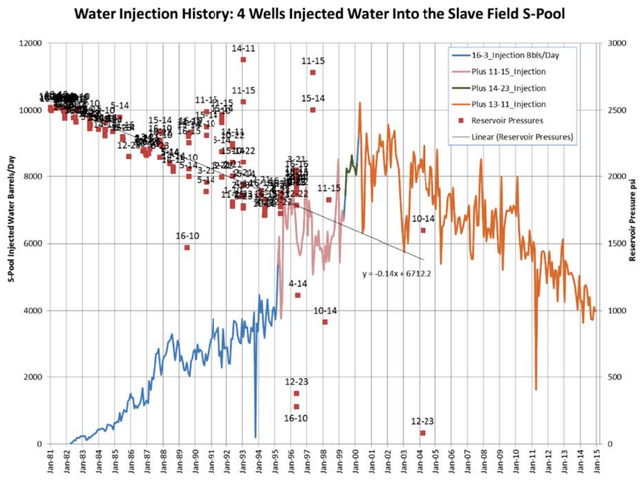

Water has been injected into the reservoir, below the oil-water contact, throughout the history of the field. Reservoir pressures record progressive pressure drop as oil is withdrawn and water is re-injected..

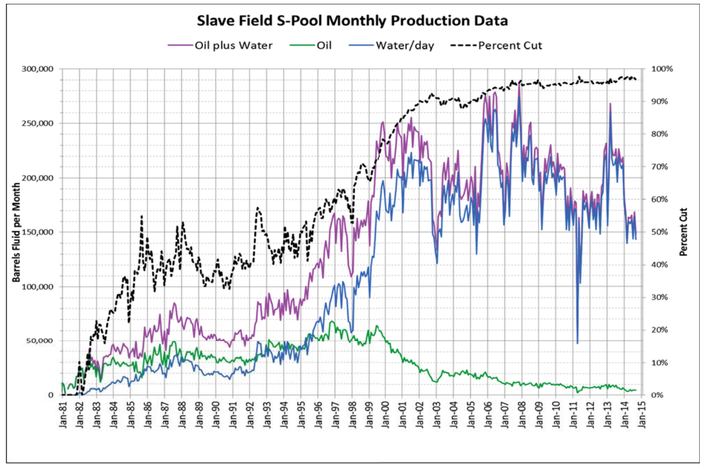

Water cut rose above 10% after only one year of production. Initial response was to increase pumping rate in order to maintain monthly oil production numbers. Result was further increase in water cut. The faster the wells are pumped, the greater the volume of water that is drawn into the wells. Although not shown on the plot, Gas:Oil ratio has remained close to its average of 235 scf/barrel throughout the history of the field. The gas is solution gas that is dissolved in the oil at reservoir pressure.

Production, injection, and pressure data document presence of an interconnected network of moldic pores within otherwise impermeable microcrystalline dolomite matrix. Molds formed where original calcite fossil fragments were encased in microcrystalline dolomite matrix, and where corrosive fluids were able to make contact with the calcite grains. Contact was made along a reaction front that propagated through the rock by leaching of fossil fragments and by "jumping" from one reactive grain to another wherever the reactive grains were touching one another. Fractures along stylolites also facilitated migration of the reaction front through the impermeable microcrystalline dolomite matrix.

The reaction front is analogous to the propagation of a flame from one flammable twig to another. Unleached calcite fossils are analogous to isolated twigs that were not contacted by the flame front.

See the cores!

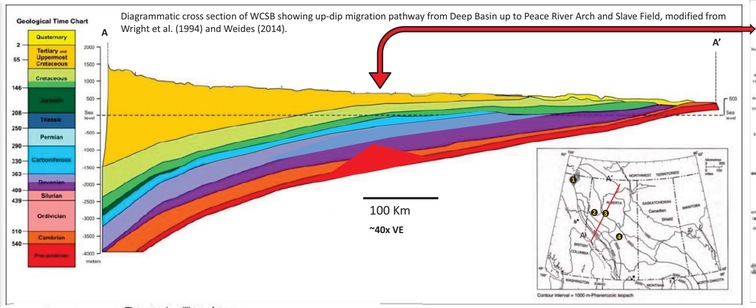

Diagrammatic cross section of WCSB showing up-dip migration pathway from Deep Basin up to Peace River Arch and Slave Field, modified from Wright et al. (1994) and Weides (2014).

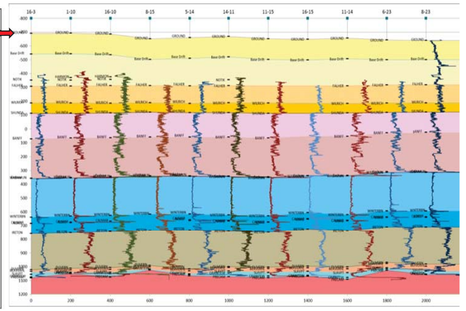

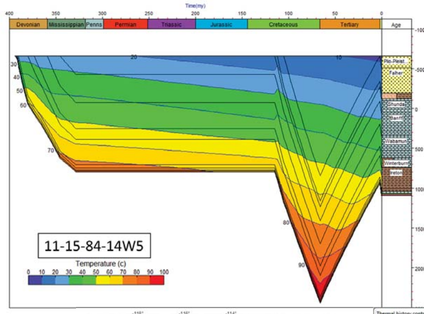

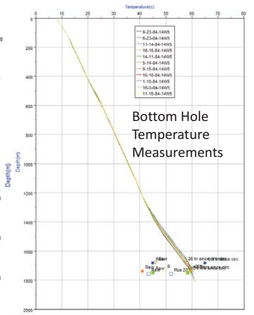

Bottom Hole Temperature Measurements

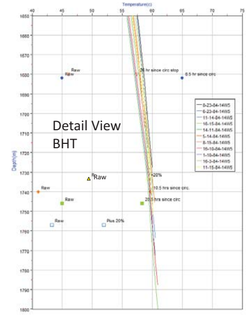

Detail View BHT

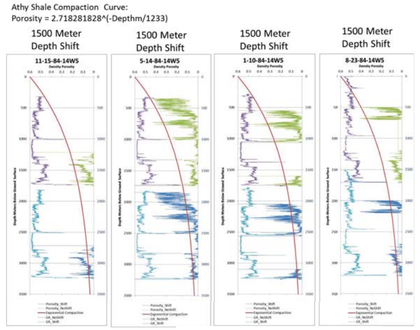

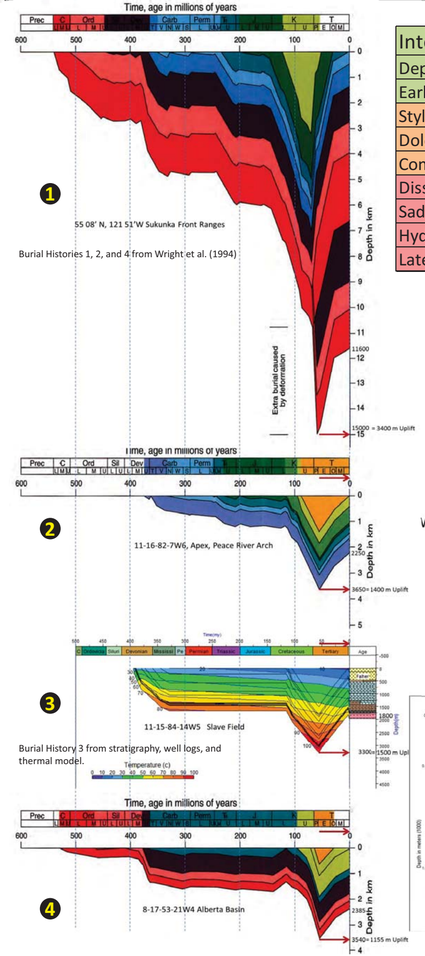

Burial Histories 1, 2, and 4 from Wright et al. (1994)

Burial History 3 from stratigraphy, well logs, and thermal model.

Interpreted Paragenetic Sequence	Early	Mid Burial	Deep Burial
Deposition of Carbonate Grains and Mud			
Early Calcite Cementation			
Stylolitiztion			
Dolomite Replacement of Micrite, but not fossil fragments			
Compaction Fracturing			
Dissolution of calcite fossil fragments, but not dolomicrite matrix			
Saddle Dolomite Cementation			
Hydrocarbon Migration			
Latest Calcite Cementation			

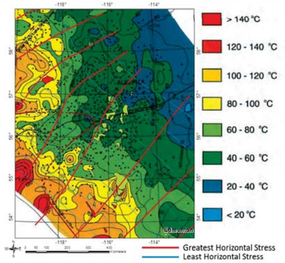

Temperature and Stress Orientation at Precambrian Surface
(Temperature from Bacu and Burwash, 1994; Stress from Bell, et al., 1994)

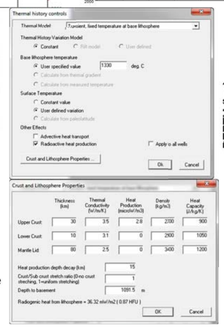

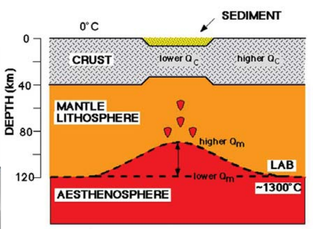

Zhiyong He ZetaWare, Inc.
Thermal-history model is based on depth to Moho of about 40 Km.

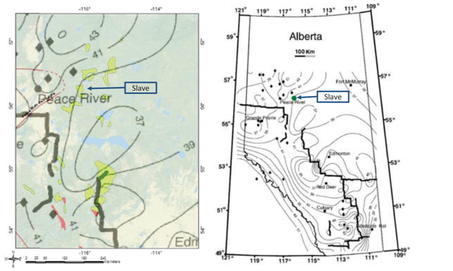

Depth to Moho in Kilometers from Bouzidi et al. (2002)

Summary:

1) Onlap of Basement Highs, less fossiliferous facies in lows, more fossiliferous facies on flanks of highs. Shale downlaps on Maximum Flooding Surface at Top Slave Point Carbonate.

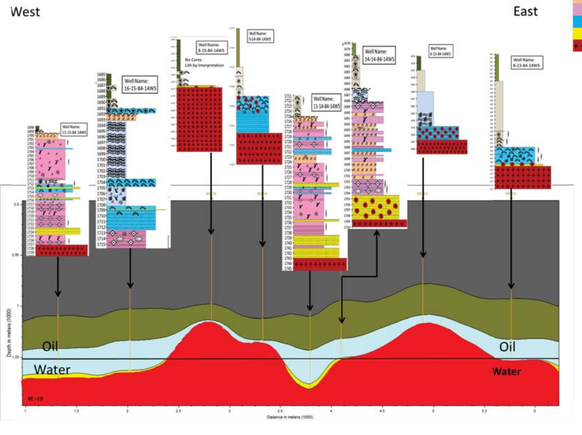

2) Burial and relatively early replacement of lime micrite by microcrystalline dolomite, followed by further burial and stylolites, followed by deeper burial and leaching of fossil fragments. Result is a carbonate reservoir of fossil molds encased in impermeable microcrystalline dolomite matrix.

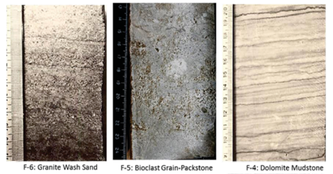

3) Generation and migration of oil. Potential source rocks are immature in Slave Field region due to inadequate burial depth. Generation took place in more-deeply buried kitchens located to the southwest. Creaney et al (1994) estimate timing of peak generation and migration is Late Cretaceous. Since oil is reservoired in moldic pores, dissolution of fossils must have taken place prior to Late Cretaceous.

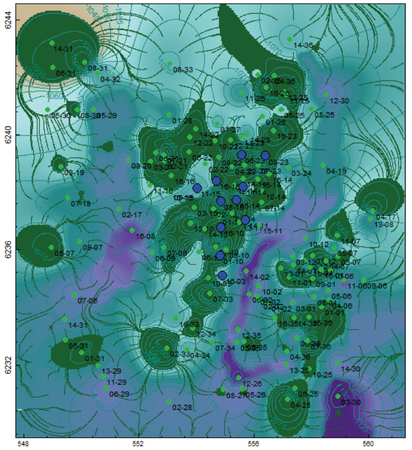

4) Discovery of Slave Field and Initial Oil Production from Water Drive Reservoir.

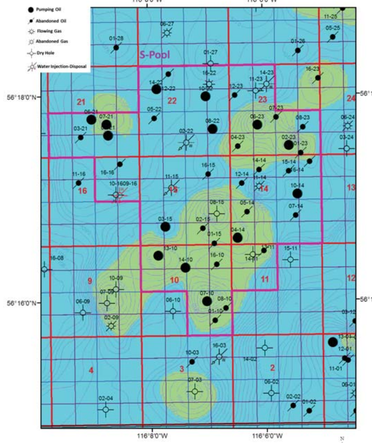

Base Slave Point Reservoir

5) Onset of high water production, sooner in some wells than in other wells.

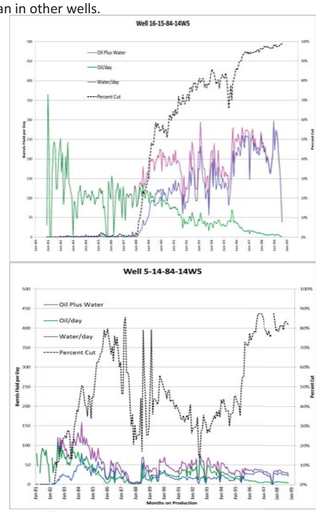

ACKNOWLEDGEMENTS:

We are grateful to the current right-holder, Penn West Petroleum, for providing data from Slave Field; particular thanks to Steve Charbonneau and Shpetim Cobaj. Additional regional data came from geoSCOUT. We thank all of the staff of the AER Core Research Centre for their superb facilities and assistance. The seismic line shown was originally acquired by Union Oil Company of Canada, and was published by Ruth M. Ferry in the CSPG Geophysical Atlas of 1989. Basin Models based on Zetaware-Genesis/Trinity.